

Analysis of Chemical Constituents of Miao Ethnomedicine Heiguteng Zhuifeng Huoluo Capsule (HZFC) and the Discovery of Active Substances in the Treatment of Rheumatoid Arthritis

Kai-lang Mu, Lei Li, Yun Chen, Min-jie Zhang, Tian-lin He, Kai-min Li, Yu-chen Liu,* and Gang Liu*



Cite This: *ACS Omega* 2024, 9, 10860–10874



Read Online

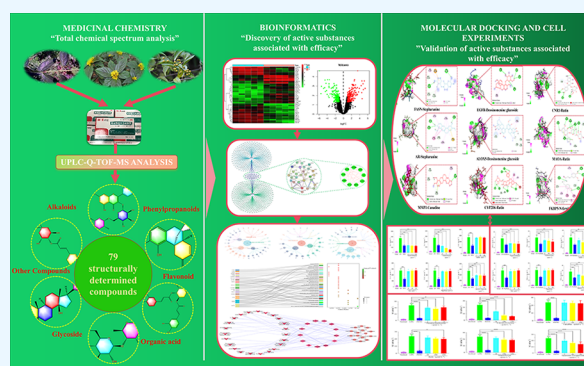
ACCESS |

Metrics & More

Article Recommendations

Supporting Information

ABSTRACT: In this study, the chemical substances of Heiguteng Zhuifeng Huoluo Capsule (HZFC) and its potential active ingredients for the treatment of rheumatoid arthritis (RA) were characterized and analyzed by medicinal chemistry combined with bioinformatics methods. Also, the potential active ingredients of HZFC against RA were verified by lipopolysaccharide (LPS)-induced macrophage activation model. The results showed that 79 chemical constituents were successfully identified, mainly including phenylpropanoids, flavonoids, and alkaloids. Among them, 13 active components were closely related to the nine core targets (FASN, ALOX5, EGFR, MMP1, CYP2D6, CNR1, AR, MAOA, and FKBP5) of HZFC in the treatment of RA. Molecular docking further proved that 13 active components had strong docking activity with 9 core targets. In the verification experiment of the LPS-induced RAW 264.7 macrophage model, the verified components (magnoflorine, *N*-feruloyltyramine, canadine, rutin, quercetin-3-*O*-glucoside, and pseudocolumbamine) all showed a clear inhibitory effect on the secretion of inflammatory factors in model cells. The above research results suggest that 13 components such as stephananine, rutin, quercetin-3-*O*-glucoside, corydine methyl ether, canadine, 8-oxoepiberberine, disinomenine, deosinomenine glucoside, tuduranine, magnoflorine, isosinomenine, pseudocolumbamine, and *N*-feruloyltyramine may be the main active substances of HZFC in the treatment of RA.



1. INTRODUCTION

Rheumatoid arthritis (RA) is an autoimmune disease characterized by chronic progressive joint disease.¹ It is characterized by multijoint, symmetrical, and invasive joint inflammation of the small joints of the hand and foot, often accompanied by extra-articular organ involvement and positive serum rheumatoid factor, which can lead to joint deformity and loss of function and even permanent disability.^{2,3} RA is particularly common in women aged 40–60 years, and its incidence is 2–3 times higher than that in men.⁴ According to the Global Burden of Disease (GBD) study, the global prevalence of RA is 0.27%, of which the highest prevalence of RA in North America and Western Europe is 0.38 and 0.35%, respectively.⁵ The actual cause of RA is still unknown. The current RA therapy mainly achieves the purpose of treatment by controlling the inflammation of joints and other tissues, maintaining joint function, preventing deformity, and repairing damaged joints.^{6–8} In recent years, the development of ethnic drugs characterized by multicomponent, multichannel, and multitarget therapy has provided a representative method for the treatment of RA.⁹

Heiguteng Zhuifeng Huoluo Capsule (HZHC) is a large variety of Miao Ethnomedicine used for cold arthralgia syndrome for many years. Since its listing, the market share of

this product ranks among the forefront of similar products. It is one of the representative drugs for the treatment of RA. The efficacy of traditional Chinese medicine is to dispel wind and remove dampness, dredge collaterals, and relieve pain. It is mostly used for wind-cold-dampness arthralgia and shoulder-arm-waist-leg pain and is especially good at treating RA disease.^{10–12} HZFC is composed of three Miao Ethnomedicine, namely, *Periploca forrestii* Schltr., *Sinomenium acutum* (Thunb.) Rehder & E.H.Wilson, and *Lysimachia paridiformis* var. *stenophylla* Franch. Among these *P. forrestii* is the rhizome of the southwest *Periploca sepium* Bunge of the Asclepiadaceae family, which has the effect of soothing tendons to activate blood, dispelling wind to eliminate dampness, and clearing heat and dispelling toxic materials.¹³ *S. acutum* is the stem of *S. acutum* (Thunb.) Reld. etWils. or *S. acutum* (Thunb.) Reld. etWils. var. *cinereum* (Diels)Reld. etWils, family Menispermaceae.

Received: December 11, 2023

Revised: February 8, 2024

Accepted: February 9, 2024

Published: February 22, 2024



ceae, and has the effect of dispelling wind-dampness, soothing meridian and collateral, and facilitating urination.¹⁴ *L. paridiformis* is the whole grass or root of Primulaceae narrow-leaved plum, which has the effects of dispelling wind and dredging collaterals, activating blood, and relieving pain.¹⁵ At present, there are only content determination and thin layer identification of single index components of sinomenine in HZFC quality control items.¹⁶ The detection index is single and has no strong correlation with efficacy, so it is difficult to control the quality of preparations, and unstable events of clinical efficacy occur frequently.^{17,18}

There are a large number of compounds in natural medicines and a wide variety of chemical structures. How to accurately identify its many components is still a challenge. Chromatographic columns and mass spectrometry detectors are complex and sensitive. The combination of liquid chromatography (LC) and high-resolution quadrupole time-of-flight (QTOF) mass spectrometry (MS) has become an indispensable tool for the detection and identification of plant secondary metabolites.^{19–21} The successful completion of the human genome project has promoted the prosperity of systems biology and bioinformatics.²² At the same time, it has also created a more systematic and rapid opportunity for revealing the material basis and mechanism of RA therapeutic drugs. The complexity of traditional Chinese medicine components leads to the diversity of their targets. The elucidation of the molecular mechanism of traditional Chinese medicine has become a bottleneck that needs to be solved urgently in the modernization and internationalization of traditional Chinese medicine. The application of molecular docking in the study of the mechanism of action between active components of traditional Chinese medicine and target proteins. Molecular docking technology is used to dock known small molecular active substances with related target proteins, which can clarify the mechanism of action between effective components of traditional Chinese medicine and targets at the molecular level.^{23,24} At present, molecular docking technology plays an important role in elucidating the mechanism of action of related target proteins in the research fields of traditional Chinese medicine active ingredients and cardiovascular diseases, cancer, and many other diseases.^{25,26} At present, the commonly used animal models of RA include the collagen-induced arthritis (CIA) model, adjuvant arthritis (AA) model, and cell models, which include synovial cells, macrophages, dendritic cells, etc.^{27–29} These models play an important role in exploring the pathogenesis of rheumatoid arthritis and the effect of drug treatment. Among them, the LPS-induced RAW 264.7 macrophage model is one of the most commonly used in vitro models for osteoclast and inflammation research and is widely used in rheumatoid arthritis research.^{30,31}

In this study, ultraperformance liquid chromatography-Q-TOF-MS (UPLC-Q-TOF-MS) technology was used to identify and characterize the chemical composition of HZFC. Further, bioinformatics and molecular docking methods were used to analyze and preliminarily verify the potential active ingredients of HZFC against RA. Finally, the analysis and prediction results were confirmed by the LPS-induced RAW 264.7 macrophage model. Our results may provide new reliable insights into the clinical application and quality control indicators of HZFC.

2. MATERIALS AND METHODS

2.1. Apparatus. An Acquity UPLC H-Class ultrahigh-performance liquid chromatograph, Xevo G2-S tof time-of-flight

mass spectrometer, Masslynx V4.1 data processing system, and UNIFI 1.7 data analysis system were all from Waters (Taunton, Massachusetts). An MS205DU type one hundred thousandth electronic balance from HSBC Mettler Toledo Instruments Co., Ltd. (Beijing, China). A SB-4200DTD ultrasonic cleaning machine was purchased from Ningbo Nianzhi Ultrasonic Equipment Co., Ltd. (Ningbo, China). A Multiskan FC microplate reader is a product of Semmerfeld Technology Co., Ltd. (Massachusetts).

2.2. Drugs and Reagents. Heiguteng Zhuifeng Huoluo Capsule (Lot: 200803) was purchased from Tongjitang Pharmaceutical Co., Ltd. (Guiyang, China). Methanol (Lot: 20201210) was purchased from Tianjin Fengchuan Chemical Reagent Technology Co., Ltd. (Tianjin, China). Rat Nitric Oxide Kit NO (Lot: 210311R05) was purchased from Sufia Biotechnology Co., Ltd. (Jiangsu, China); TNF- α ELISA kit (Lot: L210507091) and IL-6 ELISA kit (Lot: L210506259) were purchased from Wuhan Yunclone Technology Co., Ltd. (Wuhan, China). Chromatographic acetonitrile (Lot: 203319) was purchased from Seymour & Fisher Technologies Inc. (Massachusetts); lipopolysaccharide (Lot: 12181202), formic acid (Lot: 166511), and pyrrolidine dithiocarbamate (Lot: 5108–96–3) were purchased from Sigma, Inc. (St. Louis). Wahaha pure water was purchased from Hangzhou Wahaha Group Co., Ltd. (Hangzhou, China). Magnoflorine (Lot: PRF23032002), N-feruloyltyramine (Lot: PRF22082933), canadine (Lot: PRF8050941) were purchased from Chengdu Prefa Technology Development Co., Ltd. (Chengdu, China). Rutin (Lot: CHB201103) and quercetin-3-O-glucoside (Lot: CHB180628) were purchased from Chengdu Keloma Biotechnology Co., Ltd. (Chengdu, China). Pristimerin (Lot: 20200104) and pseudocolumbamine (Lot: X09S10L97258) were purchased from Shanghai Yuanye Biotechnology Co., Ltd. (Shanghai, China). The purities of all of the above reference substances were more than 98%.

2.3. Chemical Composition Analysis of HZFC.

2.3.1. Preparation of Test Solution. HZFC 1 g was placed in a 50 mL conical flask, 30 mL of 70% methanol (v/v) was added, fully infiltrated, extracted for 30 min under ultrasonic 200 W power, and filtered. The filtrate, 10 mL, was diluted 25 times with water and filtered with a 0.22 μm microporous organic filter membrane to obtain the test solution.

2.3.2. Chromatographic Condition. A BEH C18 column (2.1 mm \times 50 mm, 1.7 μm , Waters), mobile phase 0.1% formic acid water (A)–acetonitrile (B), detection wavelength of 210–410 nm, column temperature of 45 $^{\circ}\text{C}$, flow rate of 0.40 mL/min⁻¹, injection volume of 1 μL , and gradient elution (0–2 min, 4% A; 2–8 min, 4–18% A; 8–16 min, 18–35% A; 16–22 min, 35–38% A; 22–28 min, 38–90% A; 28–32 min, 90% A) were employed.

2.3.3. Mass Spectrometry Conditions. The mode of electrospray ionization with positive and negative ion detection was used. The capillary voltage was 2.5 kV, the cone hole voltage was 25 V, the ion source temperature was 120 $^{\circ}\text{C}$, the desolvent temperature was 400 $^{\circ}\text{C}$, the desolvent airflow rate was 1000 L h⁻¹, the scanning range was 50–1200 Da, the collision energy was 40 eV, and the scanning mode was MSE.

2.3.4. Component Analysis. The solution of the test sample under Section 2.3.1 was taken, and the samples were injected according to the chromatographic and mass spectrometry conditions under Sections 2.3.2 and 2.3.3. The chemical constituents of HZFC were identified by online database matching, analysis of the fragmentation rules of the secondary

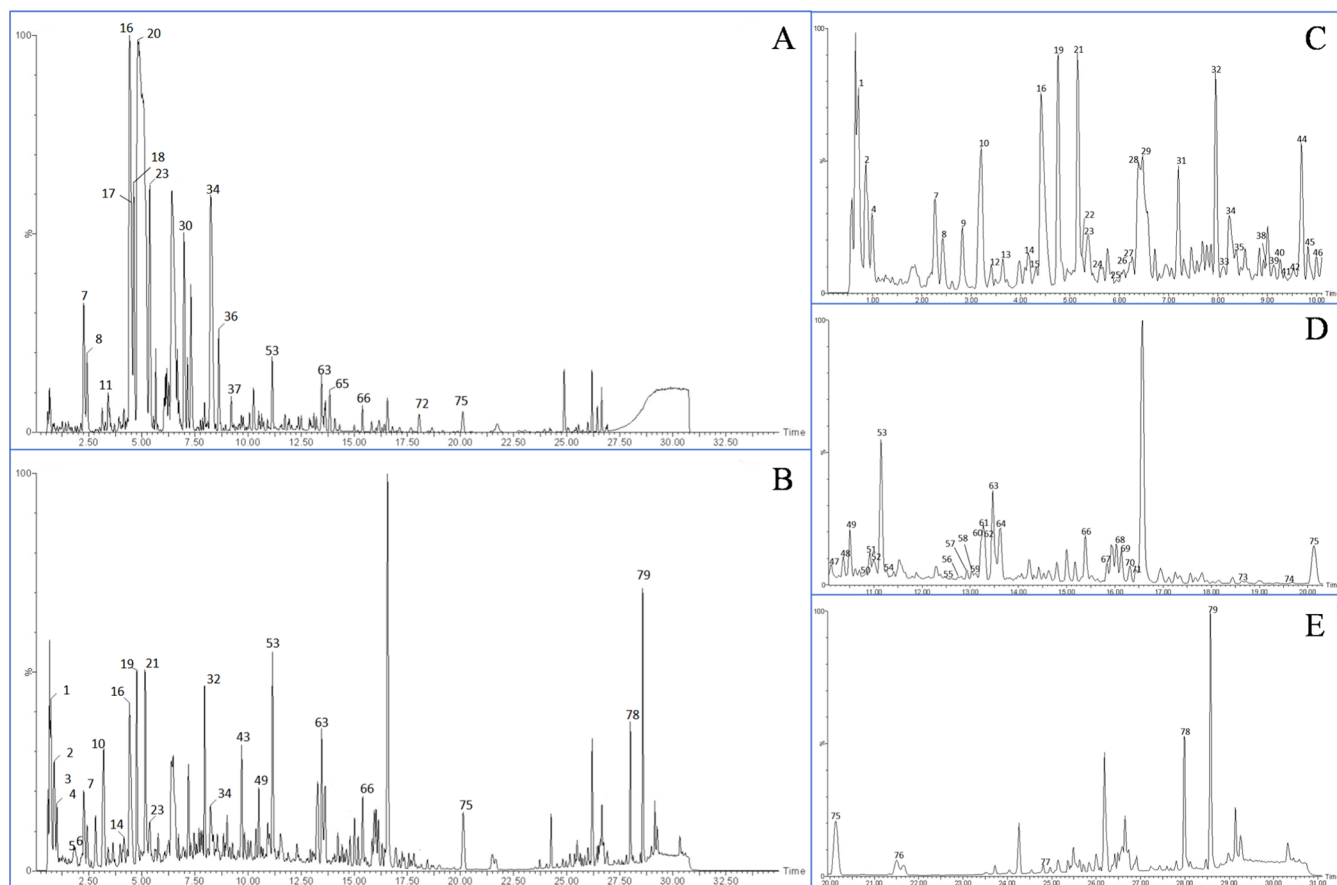


Figure 1. BPI diagram of HZFC in positive and negative ion modes: (A) positive ion mode; (B) negative ion mode; (C) 1–10 min local enlarged image; (D) 10–20 min local enlarged image; and (E) 20–31 min local enlarged image.

fragments of the chromatographic peaks, and reference to the relevant literature.

2.4. Bioinformatics Analysis. 2.4.1. RA Data Chip Search.

The Gene Expression Omnibus (<https://www.ncbi.nlm.nih.gov/geo/>) database was searched for RA gene chips with the keyword “rheumatoid arthritis”. The filtering conditions were set as Entry type was Series, Study type was Expression profiling by array, and Top Organisms was *Homo sapiens*, and the most suitable GEO data chip for RA disease was mined.

2.4.2. RA Differential Gene Analysis. The expression matrix was extracted using the GEOquery package of R software, and the gene probes and nonspecific probes containing missing values were removed and annotated according to the official Web site information. The data of the RA group (experimental group) and normal group (control group) were analyzed by the limma package. The screening criteria of differentially expressed genes (DEGs) was $\log_2 \text{FC} \geq 0.5$, $P < 0.05$. The obtained differential genes were used to draw heat maps and volcano maps using the pheatmap package.

2.4.3. Target Prediction of the Chemical Composition of HZFC. The chemical constituents identified under Section 2.3.4 were further screened using the Swiss ADME platform. The gastrointestinal absorption score was “high”, and the drug-likeness passed at least 2 “Yes”. The eligible compounds were predicted in the SwissTarget Prediction database to predict the target of each chemical component. The UniProt (<https://www.uniprot.org/>) database was used to correct the predicted targets and eliminate nonhuman genes so as to obtain the potential targets of the chemical constituents of HZFC.

2.4.4. Construction of Drug Regulatory Network and Screening of Core Targets. The drug targets and RA differential targets were intersected to obtain the drug–disease intersection targets. The intersection targets and chemical components were imported into Cytoscape software to construct the chemical composition–intersection target regulatory network of HZFC. The intersection targets were input into the String Web site to obtain the PPI interaction relationship data between the targets, which was imported into Cytoscape software, and the network was topologically analyzed using the cytoNCA plug-in. The betweenness centrality (BC) and degree centrality (DC) values of the topological index were greater than the median value as the screening condition to screen the core targets and obtain the core targets.

2.4.5. Enrichment Analysis. The core target proteins of HZFC were uploaded to the Metascape platform (<http://metascape.org/>) for Gene Ontology (GO) analysis, including three parts: biological process (BP), molecular function (MF), and cellular component (CC). The analysis results of each module were sorted according to the P value from small to large, and $P \leq 0.01$ was used as the screening condition to visualize the first five items of each module. With the help of the ClueGO plug-in in Cytoscape 3.7.2 software, $P \leq 0.01$ and κ score of 0.4 were selected to perform Kyoto Encyclopedia Genes and Genomes (KEGG) pathway analysis on the key targets of HZFC in the treatment of RA and visualize the first 30 pass results. At the same time, Cytoscape 3.7.2 software was used to construct the “active ingredient–core target–key pathway” network and visualize the results.

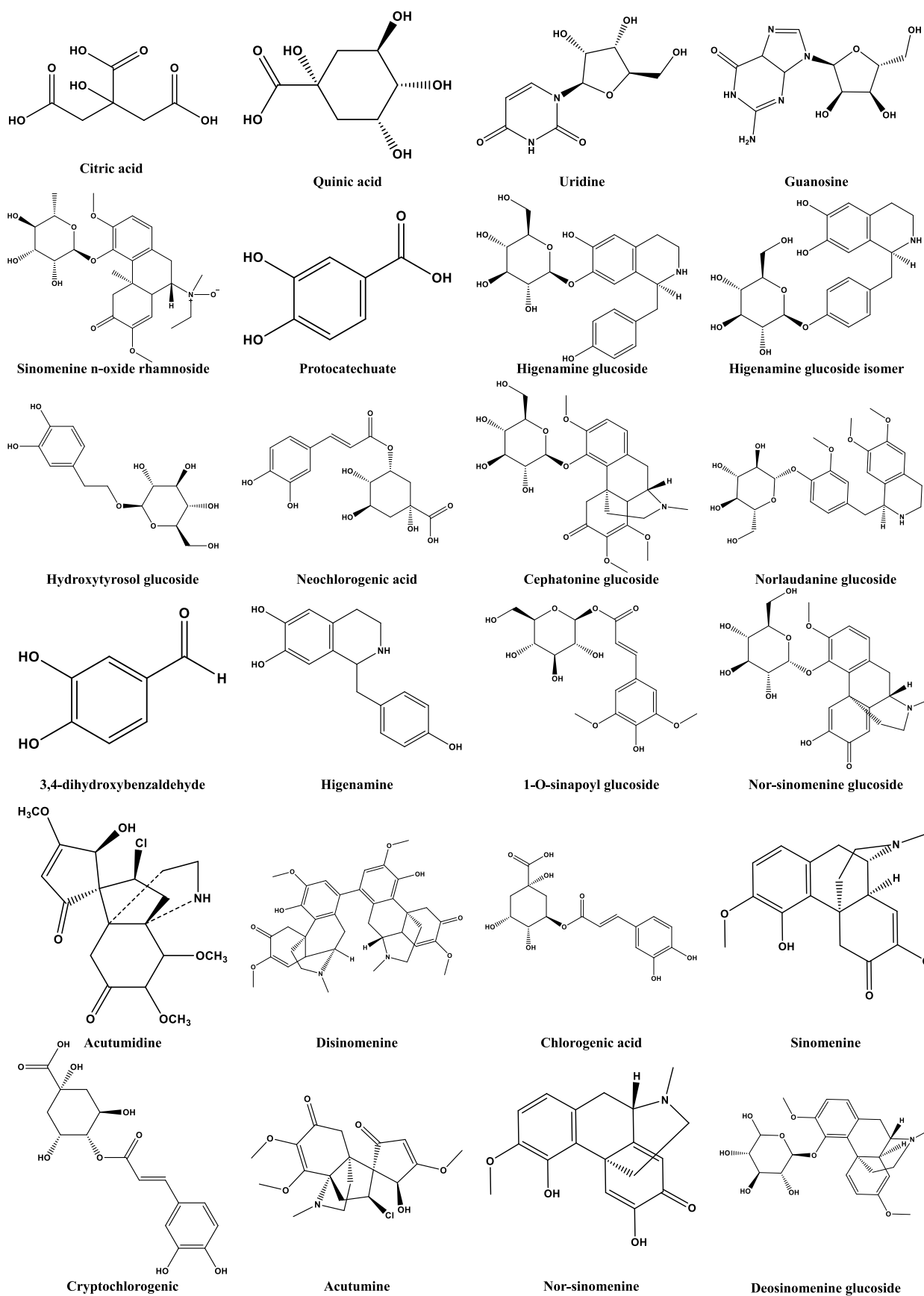


Figure 2. continued

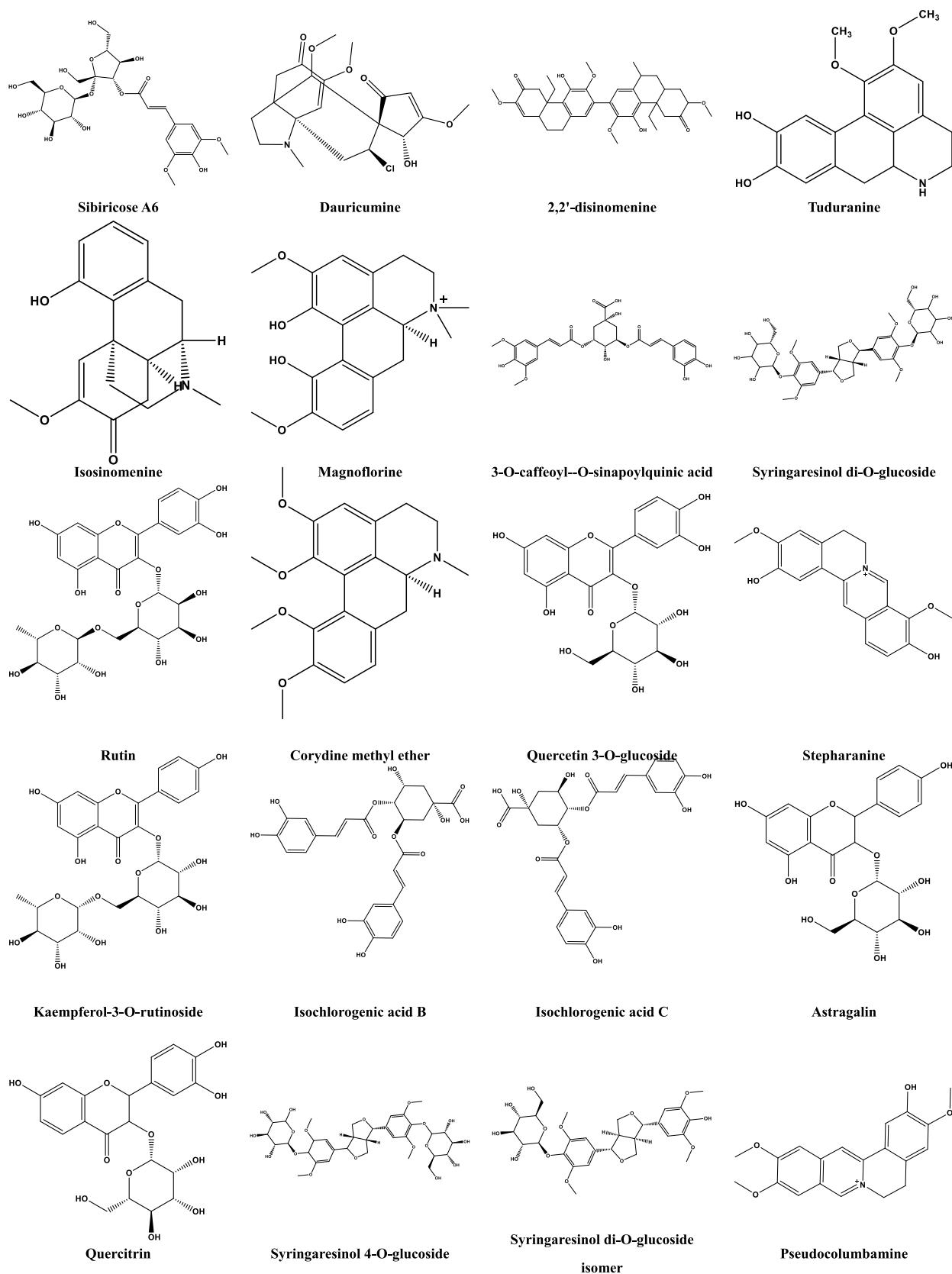


Figure 2. Structure of compounds identified in the extract of HZFC.

2.4.6. Molecular Docking. The sdf format of the active ingredient was downloaded from the PubChem Web site and then imported into the Chem three-dimensional (3D) 19.0 software to convert it into a 3D mode and save it in the mol²

format as a small molecule compound ligand. The 3D structure (pdb format) of the core target protein was downloaded from the protein structure database (PDB, <https://www.rcsb.org/>). As a receptor, SYBYL-X 2.0 software was used for batch

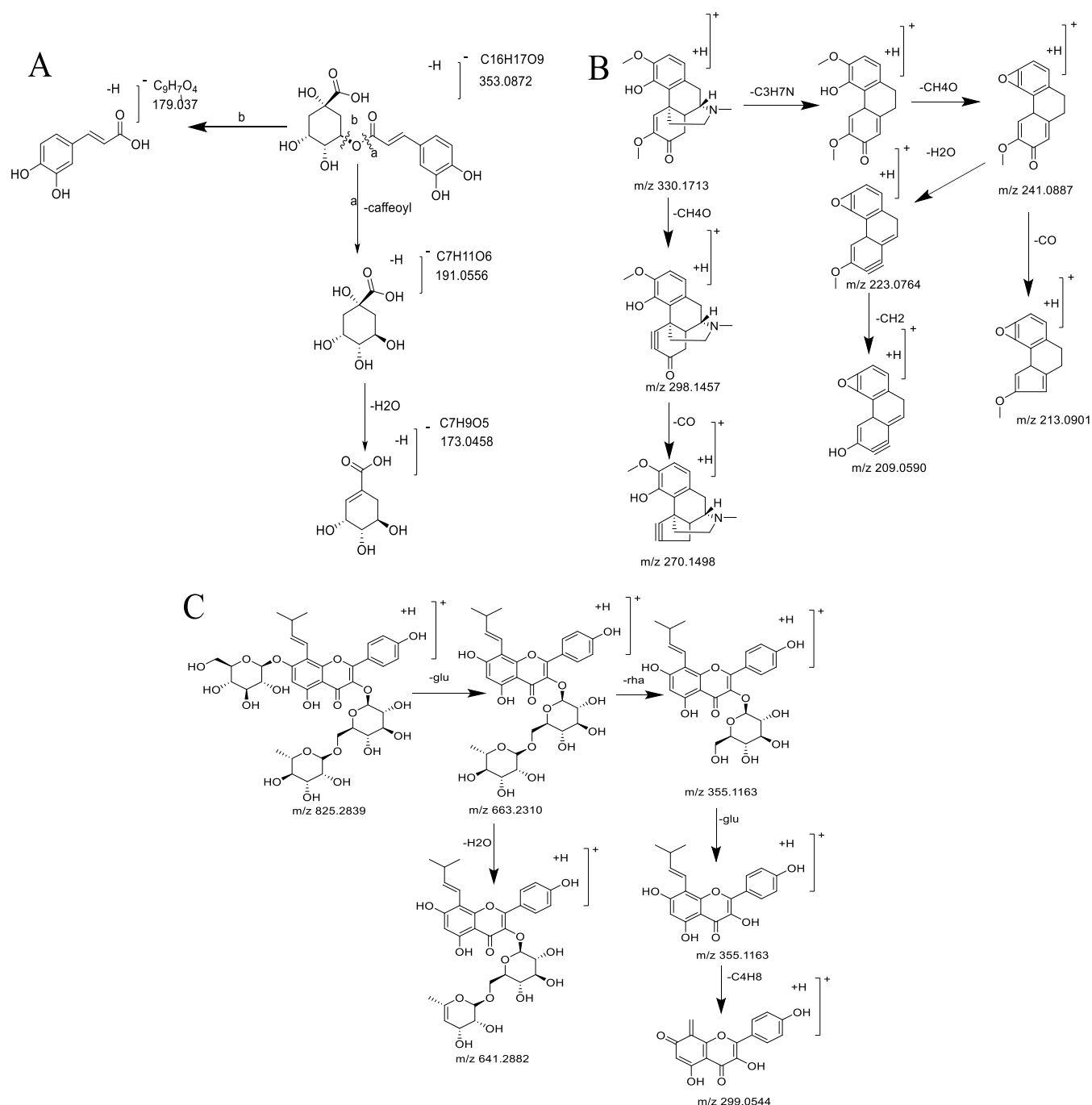


Figure 3. Cleavage pathway of main components in HZFC. (A) Main mass spectrometry fragmentation pathway of chlorogenic acid. (B) Main mass spectrometry fragmentation pathway of isatinine. (C) Main mass spectrometry fragmentation pathway of 8-prenylkaempferol-3-*O*-rutinoside.

molecular docking to verify the affinity of the active component to the core target so as to screen out the potential active components of HZFC in the treatment of RA for further experiments. Pymol and Discovery Studio software were used to visualize the docking results of some compounds and core targets.

2.5. Experimental Verification. 2.5.1. Cell Modeling, Grouping, and Administration. Bioinformatics predicted a total of 13 active ingredients. Due to the difficulty in obtaining some compounds, we collected a total of six of them. Therefore, the verification test was mainly carried out with the obtained six compounds. RAW 264.7 cells in the logarithmic growth phase

were inoculated into 96-well cell culture plates with 5×10^5 cells/mL and 100 μ L/well and cultured in an incubator with 5% CO_2 at 37 $^\circ C$ for 24 h; then, the old culture medium was discarded. In the experiment, the normal group, the model group, the positive drug group, and the sample group were set up. The normal group and the model group were added with 200 μ L of basic medium, the positive drug group was added with 200 μ L of basic medium containing different concentrations of pristimerin or PDTC, and the sample group was added with 200 μ L of basic medium containing different concentrations of compounds (six compounds including magnoflorine, *N*-feruloyltyramine, canadine, rutin, quercetin-3-*O*-glucoside, and

pseudocolumbamine were tested at multiple concentration gradients from 2×10^{-8} to 1×10^{-4} mol L⁻¹, and three multiple holes were set for each concentration; after being cultured in an incubator containing 5% CO₂ at 37 °C for 2 h, 10 μL of the basic medium was added to the normal group and 10 μL of LPS with a concentration of 20 μg mL⁻¹ was added to the other groups. After being cultured in an incubator containing 5% CO₂ at 37 °C for 24 h, the cell supernatant was centrifuged at 2500 r min⁻¹ for 10 min to remove the precipitate for later use.

2.5.2. Determination of Inflammatory Factors in Cell Supernatant. The supernatant of the above cells was taken, and the OD value was measured according to the kit instructions. NO was determined by the Greiss method, IL-6 and TNF-α were determined by the ELISA method, and the contents of NO, IL-6, and TNF-α were calculated.

2.5.3. Statistical Analysis. Statistical analysis was performed using GraphPad Prism 9.5.0 software. One-way ANOVA was used to test differences between groups. $P < 0.05$ were considered statistically significant.

3. RESULTS

3.1. Research Results of the Chemical Constituents of HZFC. The BPI diagram of HZFC in positive and negative ion modes (Figure 1) was obtained, and the compound database of three medicinal materials in HZFC was established. Then, the structure of the self-built compound database was imported into UNIFI software, and the software was used for matching. The results of software matching were corrected by combining multiple logics such as literature report, biological relationship, biosynthetic pathway, polarity size, and retention time, and the most reasonable possible or further modified structure was selected. Through the mutual confirmation of positive and negative ion modes and the attribution of secondary mass spectrometry fragments, the logical integrity of the analytical identification results was made further smooth and self-consistent, and the identification of the main chemical components in HZFC was realized. Finally, 91 main chromatographic peaks were found from HZFC, and 79 compounds were identified (Supporting Information Table S1 and Figure 2). The identified components mainly included phenylpropanoids, flavonoids, alkaloids, steroid saponins, and a small amount of nucleosides and fatty acids.

3.1.1. Phenylpropanoids. From the HZFC, the main components of *P. forrestii* were phenylpropanoids and a small amount of steroidal saponins. Among them, phenylpropanoids were abundant, mainly caffeic acid or sinapic acid and quinic acid. The ester derivatives, steroidal saponins, are mainly periplocins and their analogues.

The mass spectrometry cleavage of phenylpropanoids is mainly based on ester bond cleavage, accompanied by secondary cleavage pathways such as dehydration. A total of three components with the same molecular weight and fragment ions were found in HZFC. The quasi-molecular peak $[M - H]^-$ exact molecular weight was m/z 353.0868, and the corresponding elemental composition was C₁₆H₁₇O₉. There were two characteristic fragment ions: m/z 191.0556 and m/z 179.0537. Chlorogenic acid components were ester compounds whose hydroxyl groups of caffeic acid and quinic acid were linked by ester bonds, so their mass spectrometry cleavage was mainly based on the ester bond cleavage. The two characteristic fragments of m/z 191.0556 and m/z 179.0537 are the quinic acid anion or caffeic acid anion formed by the cleavage of the ester bond. We also found three compounds with a molecular

ion of 353.0868 in the compound, and there were two characteristic fragment ions of 191.0556 and 179.0537. Combined with the peak order reported in the literature, the 10#, 19#, and 21# compounds were identified as neochlorogenic acid (4-*O*-caffeoylquinic acid), chlorogenic acid (3-*O*-caffeoylquinic acid), and cryptochlorogenic acid (5-*O*-caffeoylquinic acid), respectively. Similarly, for 32#, 47#, and 48# compounds, the excimer ion peak $[M-H]^-$ is m/z 559.1442, the characteristic fragment ions are m/z 353.0868, m/z 191.0556, and m/z 179.0352, and the smaller fragment m/z 205.0482 can be observed. Among them, m/z 353.0868, m/z 191.0556, and m/z 179.0352 are completely consistent with the fragment ions of chlorogenic acid, and the additional m/z 205.0482 is a sinapate anion. Therefore, it can be speculated that 32#, 47#, and 48# have the same structural fragments as chlorogenic acid and also have one more sinapoyl group. Therefore, the 32#, 47#, and 48# compounds were identified as 3-*O*-caffeoyl-5-*O*-sinapoylquinic acid, 5-*O*-caffeoyl-3-*O*-sinapoylquinic acid, and 3-*O*-caffeoyl-4-*O*-sinapoylquinic acid (according to the retention time, the order may also change), respectively. The quasi-molecular ion peaks $[M - H]^-$ of the 39#, 40#, and 46# compounds were all m/z 515.1208, and the other fragment ions were completely consistent with chlorogenic acid. It can be seen that these three compounds have one more caffeoyl group than the structure of chlorogenic acid. Combined with the retention time sequence in liquid chromatography reported in the literature, 39#, 40#, and 46# were identified as isochlorogenic acid B, isochlorogenic acid C, and isochlorogenic acid A, respectively. Because neochlorogenic acid (4-*O*-caffeoylquinic acid), chlorogenic acid (3-*O*-caffeoylquinic acid), and cryptochlorogenic acid are only different from the hydroxyl link position of caffeoyl and quinic acid, the three chlorogenic acid components have the same cleavage pathway and mass spectrum. Taking chlorogenic acid as an example, the mass spectrometry fragmentation pathway of caffeoylquinic acid derivatives was illustrated (Figure 3A).

3.1.2. Alkaloids. The components identified from *S. acutum* were mainly alkaloids, and the main alkaloid structures were isoquinoline alkaloids, including a variety of subdivision structure types such as biphenanthrene-type alkaloids, morphine-type alkaloids, protoberberine type, and bisbenzylisoquinoline type. At the same time, less reported alkaloid glucosides were also found, among which sinomenine, isosinomenine, and sinomenine were high in content and strong in response. In the structure of these isoquinoline alkaloids, oxo-substitution, methoxy-substitution, or *N*-methyl-substitution are common. Therefore, the phenomena of demethylation, deoxygenation, and dehydration can be observed in the mass spectrometry cracking process of isoquinoline alkaloids, and the phenomena of de-CO, de-methanol, -CH₂O, and parent nucleus rearrangement can be further observed. The process of losing HCl can also be observed in alkaloids containing Cl atoms. Glycosyl-containing alkaloid glycosides can see the same deglycosylation process as general glycosides.

The main mass spectrometry fragmentation process of morpholine alkaloids was explained by the identification process of the 31# compound isorine. In the positive ion mode, the 31# compound obtained the molecular ion $[M + H]^+$ m/z 330.1710, and the corresponding element composition was C₁₉H₂₄NO₄. It can be seen that the molecular formula of the 31# compound is C₁₉H₂₃NO₄; the main mass spectrometry fragment is $[M + H - CH_4O]^+$ m/z 298.1457, and it is speculated that the structure contains methoxy substitution. In addition, $[M + H - C_3H_7N - CH_4O]^+$ m/z 241.0884 can be observed. Combined with the

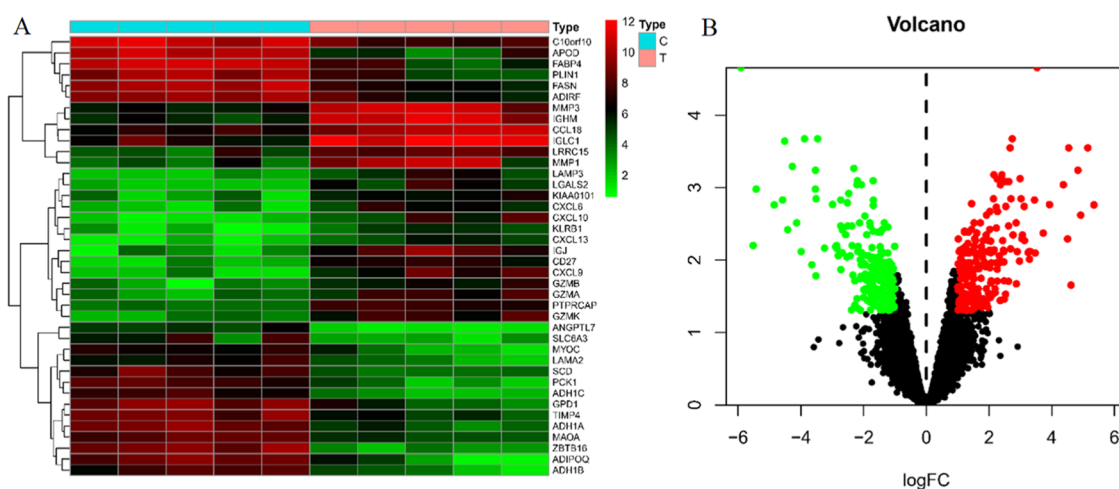


Figure 4. RA differential gene expression analysis: (A) heat map and (B) volcano map.

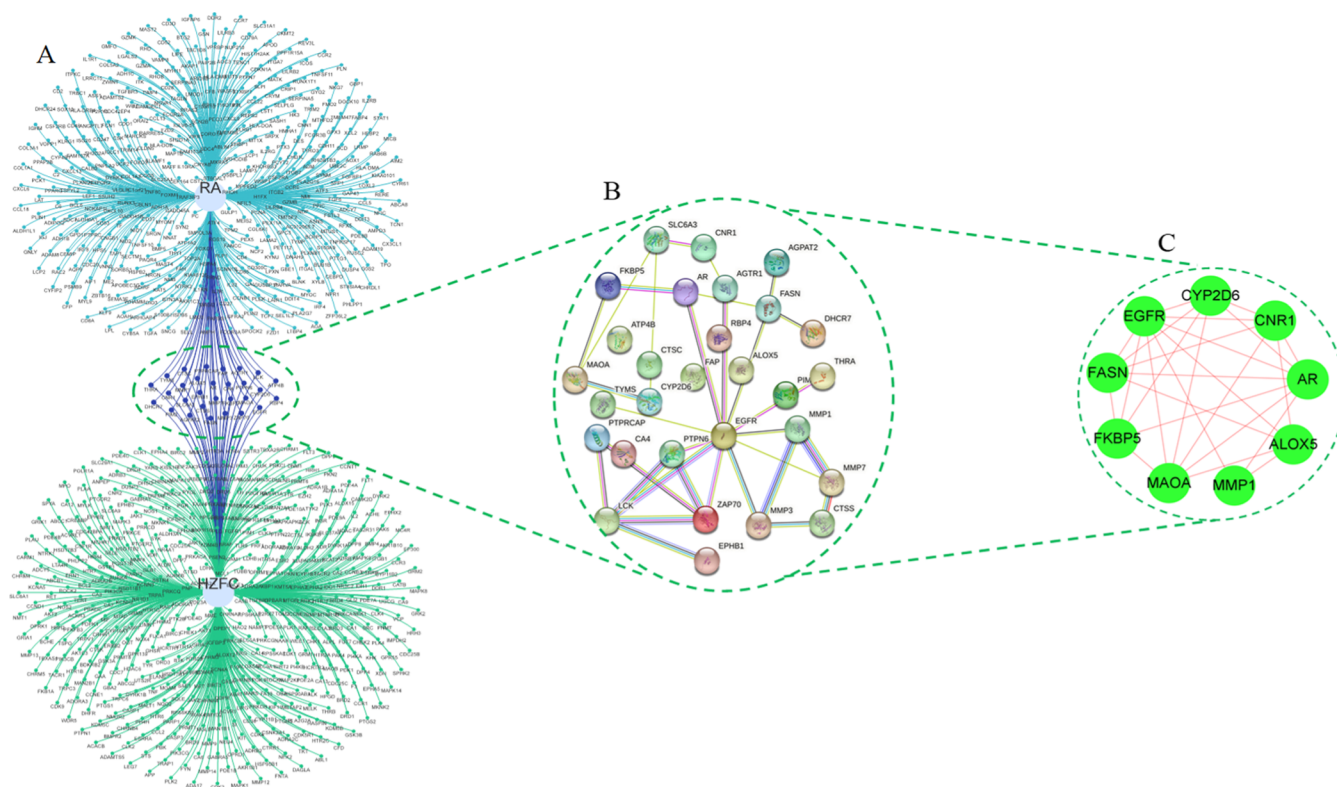


Figure 5. Drug regulatory network construction and core target screening process: (A) disease–drug intersection target map, (B) intersection target PPI interaction map, and (C) core target map.

literature, it can be seen that the characteristic C_3H_7N group is contained in the morpholine structure, and the 31# compound is identified as sinomenine (Figure 3B).

3.1.3. Flavonoids. The main components identified from *L. paridiformis* *stenophylla* Franch. are flavonoids. In addition to the common simple flavonoids such as rutin and quercetin glycosides, many characteristic components containing isopentenyl structure are also found, mainly 8-isopentenyl kaempferol and icaritin.

The flavonoids identified from HZFC are mainly flavonoid glycosides, and the main cracking process is also based on deglycosylation. The 50# compound ($t_R = 10.50$ min) has an excimer ion peak in the negative ion mode $[M - H]^-$ m/z 823.2692, and the elemental composition is calculated. The

fragment ion m/z 661.2339 $[M - H-Glu]^-$ formed by the removal of a molecule of glucose group can be observed; in the positive ion mode, the quasi-molecular ion peak m/z 825.2839 $[M + H]^+$ and the fragment ion m/z 663.2310 $[M + H-glu]^+$ formed by removing a molecule of glucose group can be observed. Also, a molecule of rhamnose group was removed to form m/z 517.1687 $[M + H-glu-rha]^+$; further, a molecule of glucosyl group was removed to form m/z 355.1163 $[M + H-glu-rha-glu]^+$, and further removal of the C4 fragment in the isopentenyl group was observed in the positive ion mode to obtain the fragment m/z 299.0544 $[M + H-Rha-2Glu-C_4H_8]^+$. The molecular ions in the positive and negative ion modes are consistent with each other, and the fragment information in the positive ion mode is more abundant. Combined with the

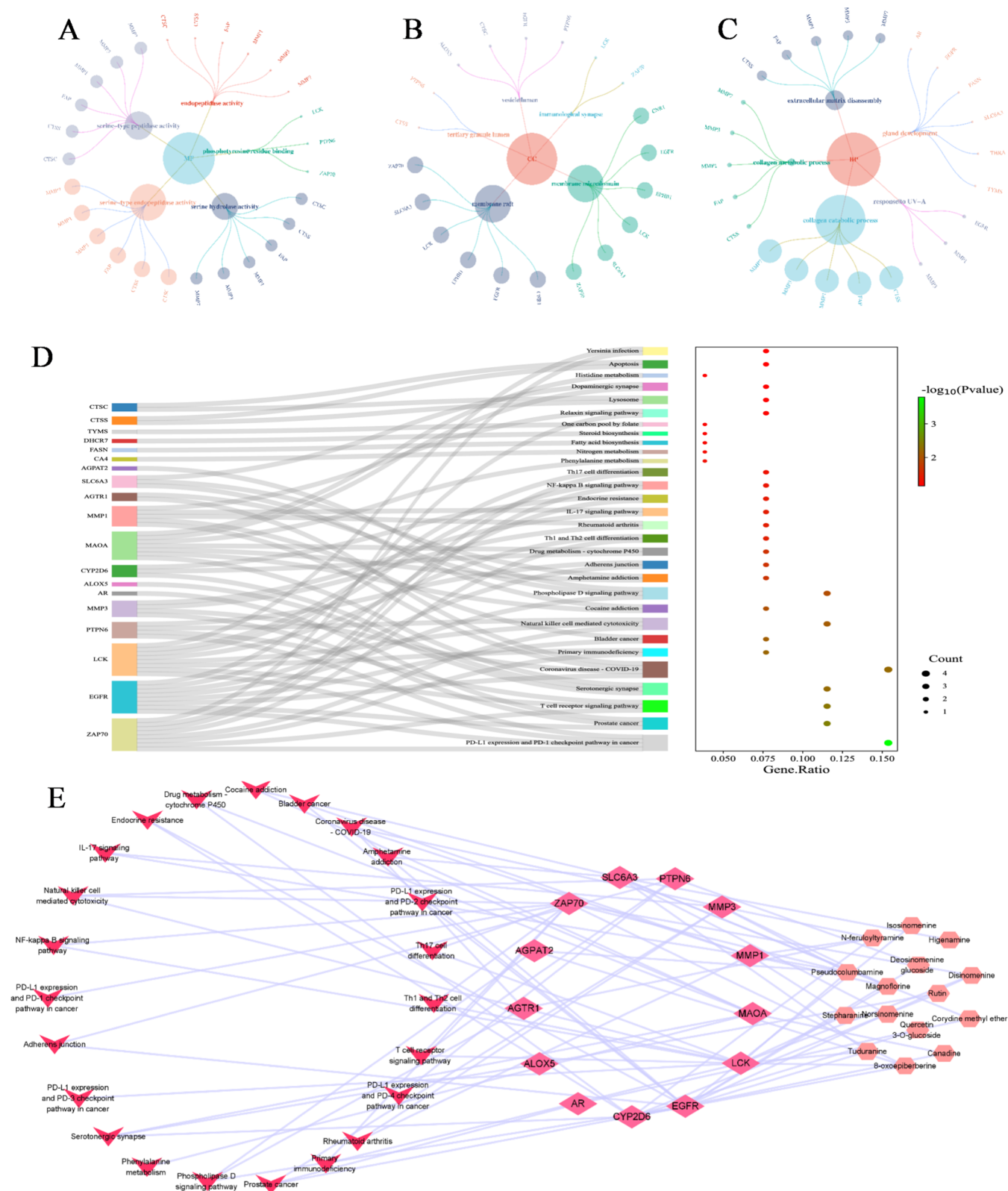


Figure 6. Enrichment analysis results: (A) MF item in the GO analysis; (B) CC item in the GO analysis; (C) BP entry in the GO analysis; (D) KEGG pathway enrichment analysis; and (E) “compound–target–pathway” network.

literature, the 50# compound was identified as 8-isopentenyl kaempferol-3-*O*-rutinose-7-*O*-glucoside (Figure 3C).

3.2. Bioinformatics Research Results. 3.2.1. RA Differentially Expressed Gene Analysis Results. The GSE1919 chip in the GEO database was screened, which included the gene

expression data of five RA subjects and gene expression data of five normal subjects. The GSE1919 chip was sorted and analyzed by R software, and the probes were screened with $\log \text{FCI} \geq 0.5$, $P < 0.05$ as the standard. A total of 428 differentially expressed genes were obtained, including 218

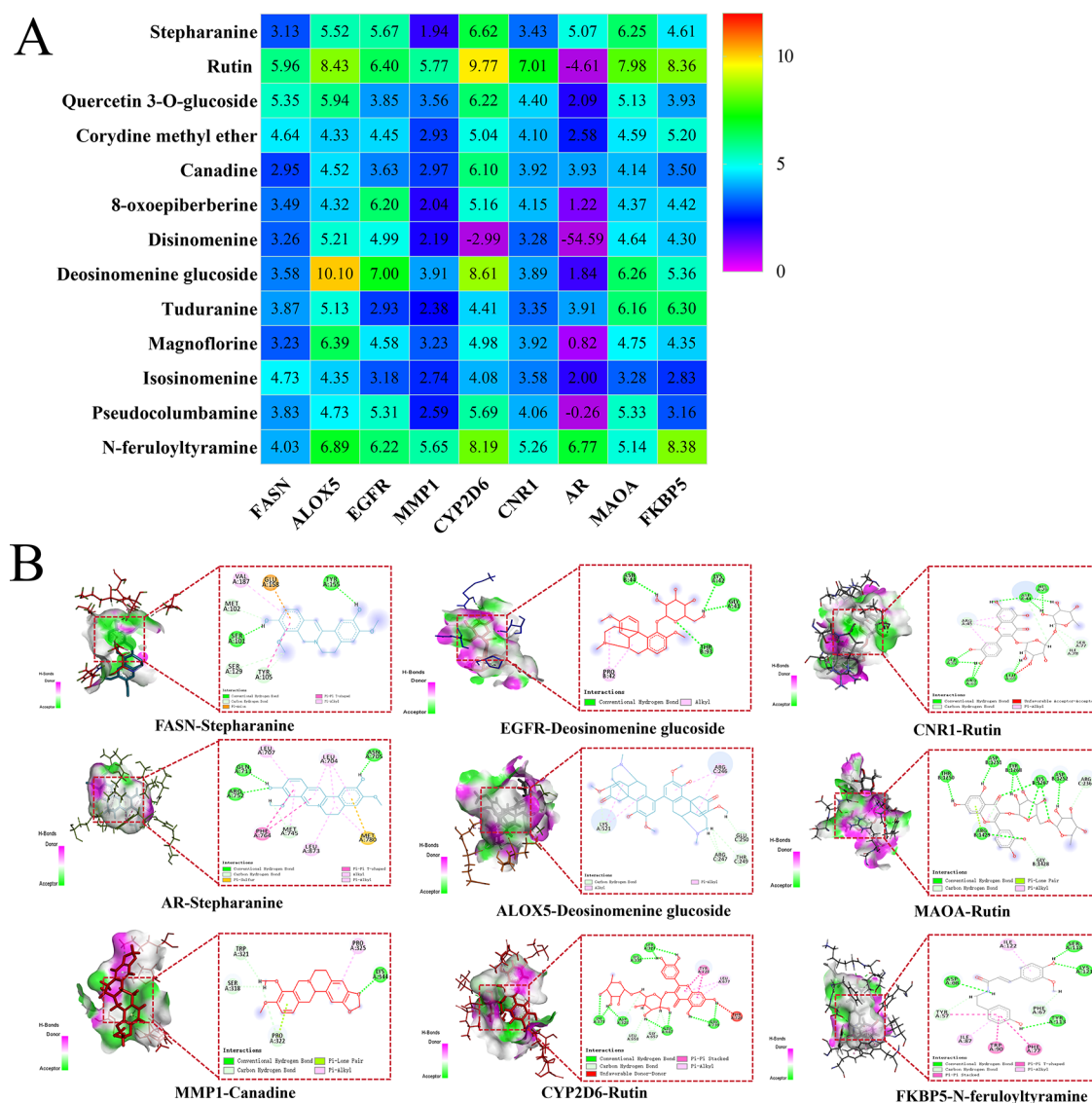


Figure 7. Molecular docking results: (A) heat map of molecular docking results and (B) molecular docking mode diagram.

upregulated genes and 210 downregulated genes. The heat maps of the top 20 genes with upregulation and downregulation (Figure 4) showed that these genes were significantly different in normal samples and RA samples.

3.2.2. Drug Target Prediction Results. The identified chemical composition smile of HZFC was imported into the Swiss ADME platform, and 26 active components were screened. The eligible compounds were predicted in the SwissTarget Prediction database, and the predicted targets were corrected using the UniProt (<https://www.uniprot.org/>) database to eliminate nonhuman genes. A total of 508 potential targets for the chemical constituents of HZFC were obtained.

3.2.3. Drug Regulatory Network Construction and Core Target Screening. The intersection of RA differential targets and active component targets of HZFC was obtained, and 29 disease–drug intersection targets were obtained (Figure 5A). The intersection target was imported into the String Web site (<https://cn.string-db.org/>) to obtain the PPI interaction network of the intersection target (Figure 5B). Further, Cytoscape software was used to screen 29 intersection targets, and a total of 9 core targets were obtained, namely, FASN,

ALOX5, EGFR, MMP1, CYP2D6, CNR1, AR, MAOA, and FKBP5 (Figure 5C).

3.2.4. Enrichment Analysis Results. GO enrichment analysis was performed using the Metascape platform with $P < 0.05$ as the screening condition. The results showed that there were 29 items related to MF. It mainly involves serine-type endopeptidase activity, serine-type peptidase activity, serine hydrolase activity, phosphotyrosine residue binding, endopeptidase activity, etc. (Figure 6A); there were 36 CC items, mainly involving membrane raft, membrane microdomain, vesicle lumen, immunological synapse, tertiary granule lumen, etc. (Figure 6B). There were 79 BP items, mainly involving collagen catabolic process, extracellular matrix disassembly, collagen metabolic process, response to UV-A, gland development, etc. (Figure 6C).

KEGG enrichment results showed that a total of 109 KEGG pathways were significantly enriched, including PD-L1 expression and PD-1, checkpoint pathway in cancer, prostate cancer, T cell receptor signaling pathway, serotonergic synapse, and coronavirus disease COVID-19 (Figure 6D). The KEGG pathway with high significance was taken as the “compound–target–pathway” network (Figure 6E).

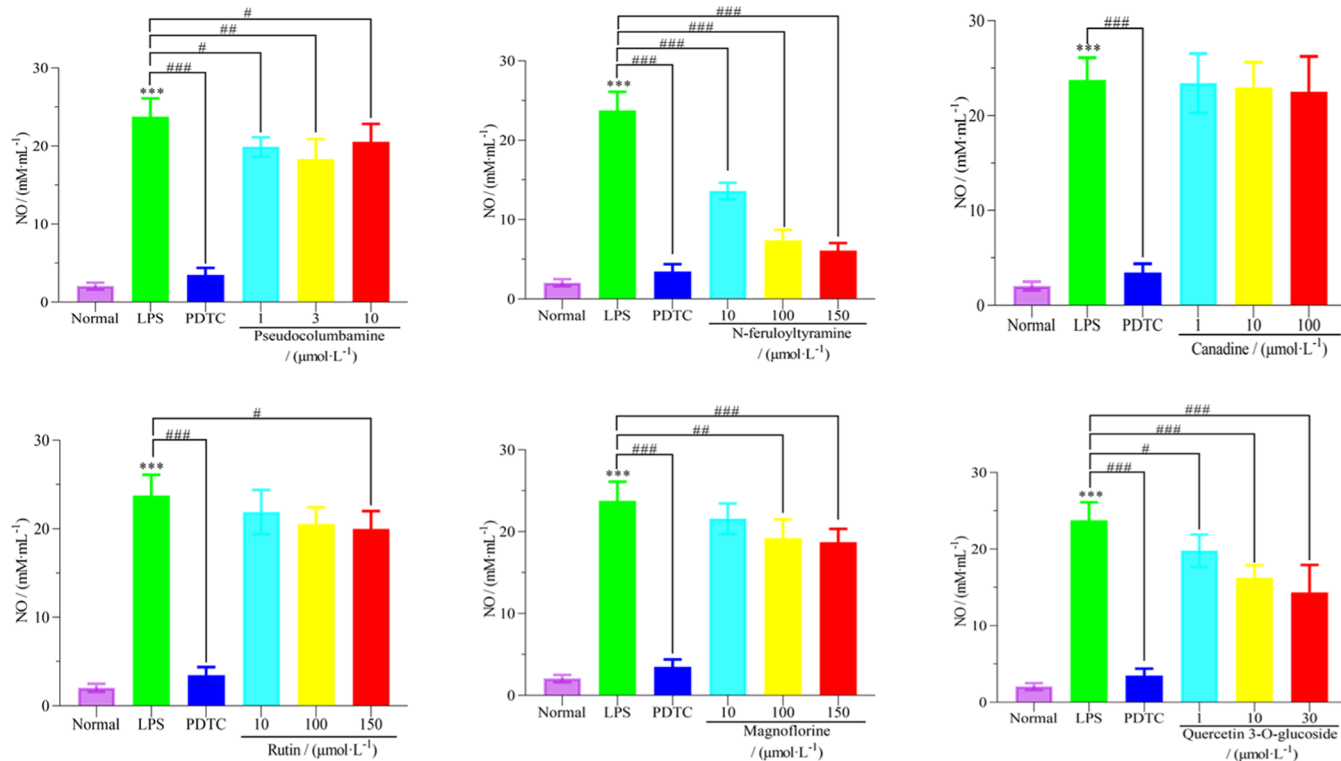


Figure 8. Effects of six compounds on the content of inflammatory factor NO in the LPS-induced RAW 264.7 cell model.

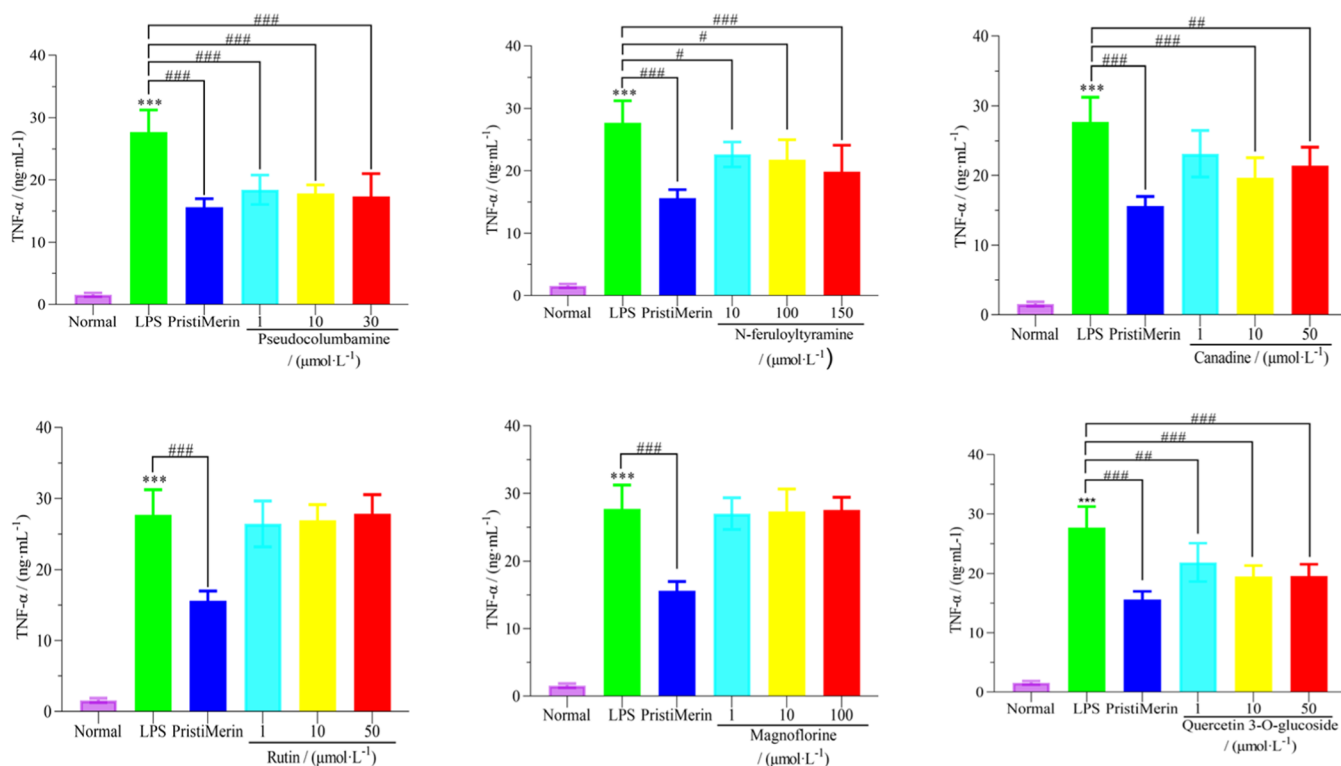


Figure 9. Effects of six compounds on the content of inflammatory factor TNF-α in the LPS-induced RAW 264.7 cell model.

3.2.5. Molecular Docking Results. The core targets screened in Section 3.2.3 were input into Section 3.2.2 to query the drug-related chemical components, and a total of 9 targets were associated with 13 active components. Molecular docking was performed using SYBYL software to obtain the docking fraction heat map of active components and target proteins, and some

molecular docking mode examples are shown in Figure 7. Among them, the greater the docking score, the better the combination of the active ingredient and the target. From Figure 7, it can be seen that most of the active ingredients can bind to the core target protein through various intermolecular forces such as hydrogen bonds.

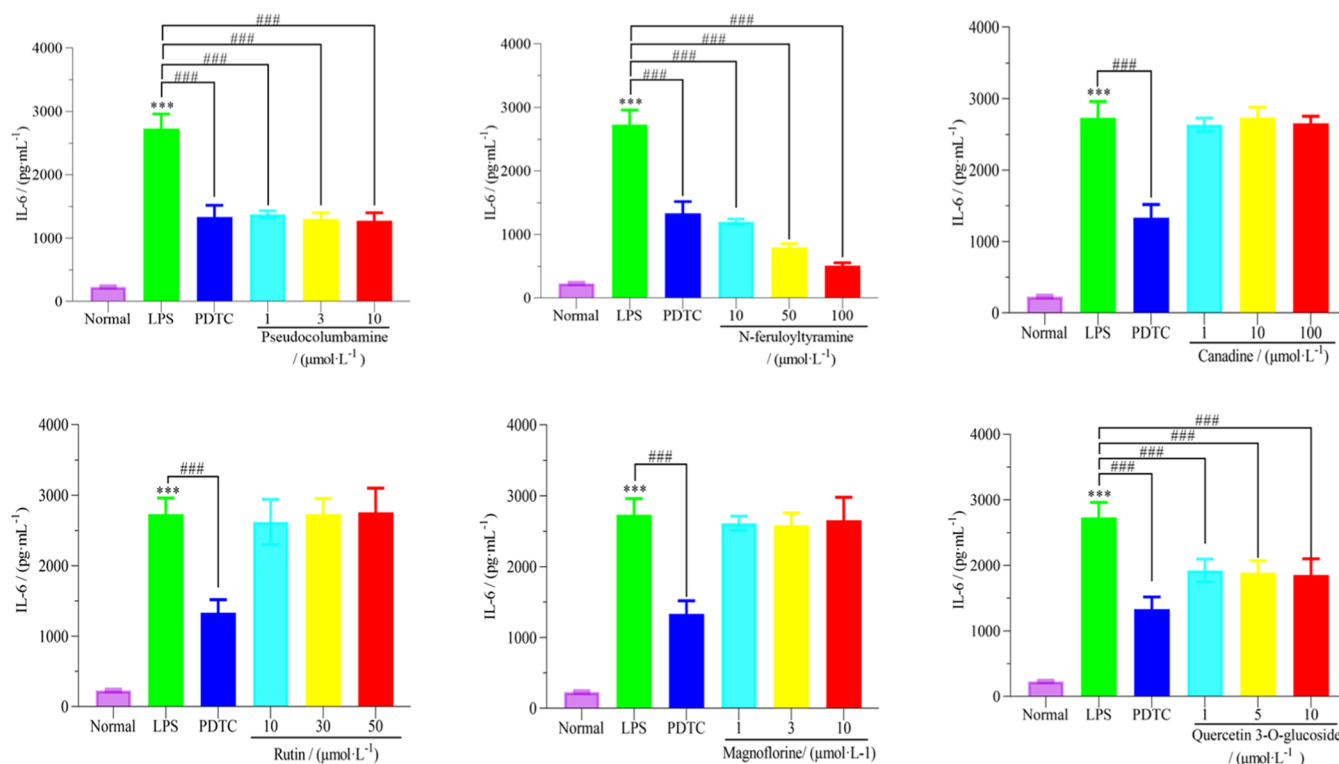


Figure 10. Effects of six compounds on the content of inflammatory factor IL-6 in the LPS-induced RAW 264.7 cell model.

3.3. Experimental Verification Results. **3.3.1. Effect of Active Ingredients on Inflammatory Factor NO in the LPS-Induced RAW 264.7 Cell Model.** The LPS-induced RAW 264.7 cell model was used to determine the effects of six active ingredients such as magnoflorine, *N*-feruloyltyramine, canadine, rutin, quercetin-3-*O*-glucoside, and pseudocolumbamine on the content of inflammatory mediator NO in the nontoxic concentration range. The results are shown in Figure 8. Among them, *N*-feruloyltyramine, quercetin-3-*O*-glucoside, and magnoflorine had a significant inhibitory effect on the expression of inflammatory mediator NO in a certain concentration range ($P < 0.001$). Pseudocolumbamine had a significant inhibitory effect on the expression of inflammatory mediator NO within a certain concentration range ($P < 0.01$). Rutin had a certain inhibitory effect on the expression of inflammatory mediator NO at higher doses ($P < 0.05$), while canadine had no significant inhibitory effect on the activity of inflammatory mediator NO in multiple concentration ranges.

3.3.2. Effect of Active Ingredients on the Secretion of Inflammatory Factor TNF- α in the LPS-Induced RAW 264.7 Cell Model. Through the LPS-induced RAW 264.7 cell model, the effects of six active ingredients, such as magnoflorine, *N*-feruloyltyramine, canadine, rutin, quercetin-3-*O*-glucoside, and pseudocolumbamine, on the content of inflammatory mediator TNF- α in the nontoxic concentration range were determined. The results are shown in Figure 9. Among them, pseudocolumbamine, *N*-feruloyltyramine, canadine, and quercetin-3-*O*-glucoside significantly inhibited the expression of inflammatory mediator TNF- α in a certain concentration range ($P < 0.001$), while rutin and magnoflorine did not inhibit the activity of inflammatory mediator TNF- α in multiple concentration ranges.

3.3.3. Effect of Active Ingredients on the Secretion of Inflammatory Factor IL-6 in the LPS-Induced RAW 264.7 Cell

Model. Through the LPS-induced RAW 264.7 cell model, the effects of six active ingredients, such as magnoflorine, *N*-feruloyltyramine, canadine, rutin, quercetin-3-*O*-glucoside, and pseudocolumbamine, on the content of inflammatory mediator IL-6 in a nontoxic concentration range were determined. The results are shown in Figure 10. Among them, pseudocolumbamine, *N*-feruloyltyramine, and quercetin-3-*O*-glucoside had a significant inhibitory effect on the expression of inflammatory mediator IL-6 in a certain concentration range ($P < 0.001$), while canadine, rutin, and magnoflorine had no inhibitory effect on the expression of inflammatory mediator IL-6 in multiple concentration ranges.

4. DISCUSSION

4.1. Analysis of the Results of Pharmaceutical Chemistry. In this study, the chemical constituents of HZFC were identified by UPLC-Q-TOF-MS, and the cleavage pathways of the main groups of compounds were discussed based on the biogenetic relationship of chemical constituents. Finally, 79 compounds including phenylpropanoids, flavonoids, alkaloids, steroidal saponins, and small amounts of nucleosides and fatty acids were identified from HZFC. Further analysis based on the literature reports showed that the morpholine-type alkaloids such as sinomenine and isatinine from *S. acutum* may be the material basis of its analgesic effect.^{32–34} The phenolic acids (phenylpropanoids) from *P. forrestii* may be the material basis of its antioxidation, promoting blood circulation and removing blood stasis.^{35–37} Flavonoids from *L. paridiformis* stenophylla Franch., especially flavonoids with prenylated structure, may have estrogenic effects similar to that of epimedium and have antiosteoporosis effects.³⁸ The results of medicinal chemistry laid the foundation for the in-depth study of the active components of Heiguteng Zhuifeng Huoluo Capsule against rheumatoid arthritis.

4.2. Bioinformatics Results Analysis. Based on the research results of the medicinal chemistry of HZFC, the intersection genes of drugs and diseases were explored, and the PPI network of intersection genes was constructed. The PPI network was further analyzed by topology analysis, and the core genes were screened by cytoNCA. The results showed that FASN, ALOX5, EGFR, MMP1, CYP2D6, CNR1, AR, MAOA, and FKBP5 had more interactions with other proteins and occupied the core position in the network. Among them, fatty acid synthase (FASN) is a key enzyme in the synthesis of fatty acids in mammals and plays an important role in the complex metabolic regulation of the body. In recent years, it has been found that the FASN gene expression is closely related to the levels of inflammatory factors IL-1 α , IL-1 β , IL-6, and IL-8.³⁹ Arachidonate 5-lipoxygenase (ALOX5) is a kind of nonheme iron dioxygenase, which is involved in the production and metabolism of fatty acid hydroperoxides. The expression of ALOX5 is closely related to the secretion of inflammatory factors.⁴⁰ Epidermal growth factor receptor (EGFR) is a member of the epidermal growth factor receptor (HER) family, which plays an important role in the physiological processes of cell growth, proliferation, and differentiation and is involved in the occurrence and repair of RA.⁴¹ Matrix metalloproteinase 1 (MMP1) is a zinc-dependent endopeptidase, which is the main protease of extracellular matrix degradation. It can degrade a variety of extracellular molecules and biologically active molecules and play a role in many biological processes, such as tissue remodeling and growth, wound repair, tissue defense mechanism, and immune response.^{42,43} Cytochrome P450D6 (CYP2D6) expression can affect the levels of TNF- α and IL-6 inflammatory factors.⁴⁴ Cannabinoid receptor 1 (CNR1) causes proinflammatory responses in macrophages, involving NLRP3 inflammasome activation and IL-1B and IL-18 secretion.⁴⁵ The main function of AR (androgen receptor) is to act as a DNA-binding transcription factor that regulates gene expression and is essential for the development and maintenance of male phenotypes.⁴⁶ Monoamine oxidase A (MAOA) is a protein-coding gene, and its related pathways include neurotransmitter release cycle and cytochrome P450 oxidation, which is involved in a variety of inflammatory processes.⁴⁷ The level of FKBP prolyl isomerase 5 (FKBP5) is closely related to the level of inflammatory factors and the ability of chondrocytes to secrete collagen.⁴⁸

The results of GO and KEGG enrichment analysis showed that the treatment of RA by HZFC mainly involved biological processes such as collagen catabolic process, extracellular matrix decomposition, and collagen metabolic process. These biological processes are usually proteolytic chemical reactions and pathways in which proteases secreted by cells lead to the decomposition of collagen in the extracellular matrix.^{49–52} It involves PD-L1 expression and PD-1 checkpoint pathway in cancer, rheumatoid arthritis, and other pathways. The PD-L1 expression and PD-1 checkpoint pathway in cancer pathway can regulate the activation, proliferation, and cytotoxic secretion of T cells and participate in the process of RA.^{53,54} Rheumatoid arthritis pathway is directly involved in the occurrence, development, and repair of the RA disease.

The results of the drug regulatory network showed that 9 core targets were closely related to 13 active components. Further molecular docking was used for preliminary verification. The results showed that rutin had strong binding activity with FASN, MMP1, CYP2D6, CNR1, and MAOA, and Deosinomenine glucoside had great binding activity with ALOX5 and EGFR. *N*-

feruloyltyramine has strong binding activity with AR and FKBP5 targets. At the same time, the results of molecular docking between 13 active components and 9 targets showed that most components had good binding activity with 9 core targets, which preliminarily proved the reliability of the analysis results.

4.3. Verification of Experimental Results Analysis. Finally, 6 of the 13 active ingredients (magnoflorine, *N*-feruloyltyramine, canadine, rutin, quercetin-3-*O*-glucoside, and pseudocolumbamine) were obtained. The six active ingredients were investigated by the LPS-induced RAW 264.7 cell model test by measuring the effects of six components on the secretion levels of inflammatory factors NO, TNF- α , and IL-6 in model cells. The antirheumatoid arthritis efficacy of the compounds was determined. The results of cell experiments showed that all six compounds had inhibitory effects on the secretion of inflammatory factors in model cells. Among them, *N*-feruloyltyramine, quercetin-3-*O*-glucoside, magnoflorine, pseudocolumbamine, and rutin have a significant inhibitory effect on the expression of inflammatory mediator NO in a certain concentration range. Pseudocolumbamine, *N*-feruloyltyramine, canadine, and quercetin-3-*O*-glucoside had a significant inhibitory effect on the expression of inflammatory mediator TNF- α in a certain concentration range. Pseudocolumbamine, *N*-feruloyltyramine, and quercetin-3-*O*-glucoside had a significant inhibitory effect on the expression of inflammatory mediator IL-6 in a certain concentration range. The seven active ingredients that have not been experimentally verified (8-oxoepiberberine, disinomenine, deosinomenine glucoside, tuduranine, isosinomenine, corydine methyl ether, and stepharanine) are alkaloids and their derivatives. Among them, 8-oxoepiberberine is a protoberberine alkaloid with rich biological activity and has shown excellent anti-inflammatory effects in various inflammatory diseases such as epilepsy and cardiovascular and cerebrovascular diseases.^{55–57} Isoquinoline alkaloids or their derivatives in *S. acutum*, disinomenine, deosinomenine glucoside, tuduranine, isosinomenine, and corydine methyl ether are isoquinoline alkaloids or their derivatives in sinomenine. It has been found that these components can act on dendritic cells to block IL-6 production and terminate Th17 cell development, thereby significantly reducing the response of encephalitis T cells and inducing the improvement of experimental autoimmune encephalomyelitis animal models. It has significant anti-inflammatory effects.^{58,59} Wang et al.³³ identified the anti-inflammatory components in *S. acutum* by spectrum–effect relationship and chemometrics methods. The results showed that stepharanine in *S. acutum* was its main anti-inflammatory component.

5. CONCLUSIONS

In summary, in this study, 79 chemical components such as phenylpropanoids, flavonoids, and alkaloids were identified from HZFC by UPLC-Q-TOF-MS, and the cleavage pathways of the main components were analyzed. Then, we used bioinformatics and molecular docking methods to preliminarily analyze and predict 13 active components closely related to the core targets of the disease, such as cepharanthine, rutin, isoquercitrin, pansythydine, tetrahydroberberine, 8-oxoepiberberine, scutellarine, deoxysinomenine glucoside, dendrobine, magnoflorine, isatinine, pseudocolumbamine, and *N*-transferuloyltyramine. Finally, we established an in vitro inflammation model of LPS-induced RAW 264.7 cells and verified the prediction results. The results showed that these 13 active components may play a major role in the treatment of RA

diseases by HZFC. Our results provide new insights into the clinical application and quality control indicators of HZFC. At the same time, there are still some limitations in this study, including the difficulty in obtaining some natural active ingredient samples and the failure to use in vivo animal models to verify the prediction results. Therefore, this part of the work still needs to be further explored.

■ ASSOCIATED CONTENT

SI Supporting Information

The Supporting Information is available free of charge at <https://pubs.acs.org/doi/10.1021/acsomega.3c09788>.

Retention time; mass spectrometry information; and identification results of chemical constituents in HZFC (PDF)

■ AUTHOR INFORMATION

Corresponding Authors

Yu-chen Liu – Guizhou University of Traditional Chinese Medicine, Guiyang 550025 Guizhou, China; orcid.org/0000-0003-0125-5067; Email: lyc8564732@163.com

Gang Liu – Guizhou University of Traditional Chinese Medicine, Guiyang 550025 Guizhou, China; Email: liugang888_2000@163.com

Authors

Kai-lang Mu – Guizhou University of Traditional Chinese Medicine, Guiyang 550025 Guizhou, China

Lei Li – Guizhou University of Traditional Chinese Medicine, Guiyang 550025 Guizhou, China

Yun Chen – Guizhou University of Traditional Chinese Medicine, Guiyang 550025 Guizhou, China

Min-jie Zhang – Guizhou University of Traditional Chinese Medicine, Guiyang 550025 Guizhou, China

Tian-lin He – Guizhou University of Traditional Chinese Medicine, Guiyang 550025 Guizhou, China

Kai-min Li – Guizhou University of Traditional Chinese Medicine, Guiyang 550025 Guizhou, China

Complete contact information is available at: <https://pubs.acs.org/doi/10.1021/acsomega.3c09788>

Notes

The authors declare no competing financial interest.

■ ACKNOWLEDGMENTS

This article is supported by the Science and Technology Top Talent Program of Guizhou Education Department (Qian teaching skill[2022]083) and Research Innovation and Exploration Project of Guizhou University of Traditional Chinese Medicine in 2021 (2019YFC1712500302). The authors thank the reviewers and editors for their sincere comments.

■ ABBREVIATIONS

RA, rheumatoid arthritis; HZFC, Heiguteng Zhuifeng Huoluo Capsule; UPLC-Q-TOF-MS, ultraperformance liquid chromatography-quadrupole-time-of-flight mass spectrometry; GBD, global burden of disease; GO, gene ontology; BP, biological process; CC, cellular component; MF, molecular function; KEGG, Kyoto Encyclopedia of Genes and Genomes; IL-6, interleukin 6; Th17, T helper cell 17; NF- κ B, nuclear factor κ -B; MAPK, mitogen-activated protein kinases; PI3K/Akt, phosphatidylinositol-3-hydroxy kinase/protein kinase B; COX-1, cyclooxygenase-1; COX-2, cyclooxygenase-2; LPS, lipopolysaccharide; PPI, protein–protein interaction networks; FASN, fatty acid synthase; ALOX5, arachidonate 5-lipoxygenase; EGFR, epidermal growth factor receptor; MMP1, matrix metalloproteinase 1; CYP2D6, cytochromeP4502D6; CNR1, cannabinoid receptor 1; NLRP3, NOD-like receptor thermal protein domain associated protein 3; TNF- α , tumor necrosis factor; IL 1B, interleukin-1 β ; IL18, interleukin 18; AR, androgen receptor; MAOA, monoamine oxidase A; P450, cytochromeP450; FKBP5, FKBP prolyl isomerase 5; PD-L1, programmed cell death 1 ligand 1; PDTC, pyrrolidine dithiocarbamate

■ REFERENCES

- (1) Grange, L.; Alliot-Launois, F. [Rheumatoid arthritis]. *Rev. Prat.* **2022**, *72* (1), 68–70.
- (2) Devauchelle-Pensec, V.; Guellec, D. [Rheumatoid arthritis]. *Rev. Prat.* **2015**, *65* (5), 719–729.
- (3) Sunderhaus, C. Living With Rheumatoid Arthritis. *Prof. Case Manage.* **2022**, *27* (1), 30–32.
- (4) Firestein, G. S.; McInnes, I. B. Immunopathogenesis of Rheumatoid Arthritis. *Immunity* **2017**, *46* (2), 183–196.
- (5) Finckh, A.; Gilbert, B.; Hodkinson, B.; et al. Global epidemiology of rheumatoid arthritis. *Nat. Rev. Rheumatol.* **2022**, *18* (10), 591–602.
- (6) Bullock, J.; Rizvi, S. A. A.; Saleh, A. M.; et al. Rheumatoid Arthritis: A Brief Overview of the Treatment. Medical principles and practice: international journal of the Kuwait University. *Health Sci. Centre* **2019**, *27* (6), 501–507.
- (7) Dariushnejad, H.; Chodari, L.; Sedighi, M.; et al. Rheumatoid arthritis: current therapeutics compendium. *Endocr. Regul.* **2022**, *56* (2), 148–162.
- (8) Singh, J. A. Treatment Guidelines in Rheumatoid Arthritis. *Rheum. Dis. Clin. North Am.* **2022**, *48* (3), 679–689.
- (9) Zhou, X. P.; Han, L.; Ye, Y. Y.; et al. [Progress on treatment of rheumatoid arthritis with ethnodrugs]. *Zhongguo Zhong Yao Za Zhi* **2017**, *42* (12), 2398–2407.
- (10) Liang, J.; Wang, Q.; Huang, W.; et al. [Heiguteng Zhuifenghuoluo capsule inhibits the expression of NF- κ B in synovial tissues of rats with collagen-induced arthritis and alleviates joint inflammation]. *Chin. J. Cell. Mol. Immunol.* **2019**, *35* (3), 193–198.
- (11) Zheng, K.; Chen, Z.; Sun, W.; et al. Hei-Gu-Teng Zhuifenghuoluo Granule Modulates IL-12 Signal Pathway to Inhibit the Inflammatory Response in Rheumatoid Arthritis. *J. Immunol. Res.* **2018**, *2018*, No. 8474867.
- (12) Zhu, C. X.; Zhou, X.; Chen, H. G. Research progress of vaccine therapy for rheumatoid arthritis. *Chin. J. Mod. Appl. Pharm.* **2020**, *37* (21), 2669–2677.
- (13) Li, X. F.; Liu, Y. C.; Liu, G.; et al. Research progress on chemical constituents and pharmacological effects of Rhizoma Nigrotella. *Chin. Tradit. Pat. Med.* **2018**, *40* (04), 904–912.
- (14) Luo, Y. Q.; Shen, X. L.; Cai, S. J.; et al. Research progress on chemical constituents and pharmacological effects of Sinomengensis sinomensis and prediction analysis of Q-Marker. *Chin. Tradit. Herb. Drugs* **2022**, *53* (03), 898–911.
- (15) Li, X. Z.; Zhang, S. N. Research progress on chemical constituents and pharmacological effects of Chasma phallus and prediction analysis of therapeutic potential. *Lishizhen Med. Mater. Med. Res.* **2021**, *32* (03), 708–711.
- (16) Liu, Z. K.; Yang, Y. T.; Chen, F. F.; et al. Research progress of rattan drugs in the treatment of rheumatoid arthritis. *Guizhou Med. J.* **2023**, *47* (07), 1023–1025.
- (17) He, T. L.; Liu, Y. C.; Liu, G. Research Progress and Quality Marker Prediction Analysis of Miao Medicine Heiguteng Zhuifeng Huoluo Capsule. *Asia-Pac. J. Tradit. Med.* **2023**, *19* (06), 86–91.

- (18) Xiong, H.; Yao, X. M.; Li, C. X.; et al. Research progress on the treatment of rheumatoid arthritis with *Periploca forrestii*. *J. Guizhou Univ. Tradit. Chin. Med.* **2021**, *43* (06), 83–87.
- (19) Chen, L.; Zhang, Y.; Zhang, Y. X.; et al. Pretreatment and analysis techniques development of TKIs in biological samples for pharmacokinetic studies and therapeutic drug monitoring. *J. Pharm. Anal.* **2023**, DOI: 10.1016/j.jppha.2023.11.006.
- (20) Han, C.; Zhang, Z.; Feng, Z.; et al. The “depict” strategy for discovering new compounds in complex matrices: Lycibarbarspermidines as a case. *J. Pharm. Anal.* **2023**, DOI: 10.1016/j.jppha.2023.10.007.
- (21) Kurilung, A.; Limjiasahapong, S.; Kaewnarin, K.; et al. Measurement of very low-molecular weight metabolites by traveling wave ion mobility and its use in human urine samples. *J. Pharm. Anal.* **2023**, DOI: 10.1016/j.jppha.2023.12.011.
- (22) Fu, Y.; Ling, Z.; Arabnia, H.; Deng, Y. Current trend and development in bioinformatics research. *BMC Bioinf.* **2020**, *21* (9), No. 538.
- (23) Kaur, T.; Madgulkar, A.; Bhalekar, M.; Asgaonkar, K. Molecular Docking in Formulation and Development. *Curr. Drug Discovery Technol.* **2019**, *16* (1), 30–39.
- (24) Pinzi, L.; Rastelli, G. Molecular Docking: Shifting Paradigms in Drug Discovery. *Int. J. Mol. Sci.* **2019**, *20* (18), No. 4331.
- (25) Qu, L.; Liu, Y.; Deng, J.; et al. Ginsenoside Rk3 is a novel PI3K/AKT-targeting therapeutics agent that regulates autophagy and apoptosis in hepatocellular carcinoma. *J. Pharm. Anal.* **2023**, *13* (5), 463–482.
- (26) Zhao, J.; Liu, Y.; Zhu, L.; et al. Tumor cell membrane-coated continuous electrochemical sensor for GLUT1 inhibitor screening. *J. Pharm. Anal.* **2023**, *13* (6), 673–682.
- (27) Choudhary, N.; Bhatt, L. K.; Prabhavalkar, K. S. Experimental animal models for rheumatoid arthritis. *Immunopharmacol. Immunotoxicol.* **2018**, *40* (3), 193–200.
- (28) Jang, S.; Kwon, E. J.; Lee, J. J. Rheumatoid Arthritis: Pathogenic Roles of Diverse Immune Cells. *Int. J. Mol. Sci.* **2022**, *23* (2), No. 905.
- (29) Poutoglidou, F.; Pourzitaki, C.; Dardalas, I.; et al. The Use of Collagen-Induced Arthritis Animal Model on Studying Bone Metabolism. *Calcif. Tissue Int.* **2020**, *107* (2), 109–120.
- (30) Hourii, J. M.; O’Sullivan, F. X. Animal models in rheumatoid arthritis. *Curr. Opin. Rheumatol.* **1995**, *7* (3), 201–205.
- (31) Duris, F. H.; Fava, R. A.; Noelle, R. J. Collagen-induced arthritis as a model of rheumatoid arthritis. *Clin. Immunol. Immunopathol.* **1994**, *73* (1), 11–18.
- (32) Liu, W. J.; Jiang, Z. M.; Chen, Y.; et al. Network pharmacology approach to elucidate possible action mechanisms of *Sinomenii Caulis* for treating osteoporosis. *J. Ethnopharmacol.* **2020**, *257*, No. 112871.
- (33) Wang, L. J.; Jiang, Z. M.; Xiao, P. T.; et al. Identification of anti-inflammatory components in *Sinomenii Caulis* based on spectrum-effect relationship and chemometric methods. *J. Pharm. Biomed. Anal.* **2019**, *167*, 38–48.
- (34) Zhao, Z. J.; Zhao, C.; Xiao, J.; Wang, J. C. Transdermal Permeation and Anti-Inflammation Activities of Novel *Sinomenine* Derivatives. *Molecules* **2016**, *21* (11), No. 1520, DOI: 10.3390/molecules21111520.
- (35) Chen, H.; Liang, Q.; Zhou, X.; Wang, X. Preparative separation of the flavonoid fractions from *Periploca forrestii* Schltr. ethanol extracts using macroporous resin combined with HPLC analysis and evaluation of their biological activities. *J. Sep. Sci.* **2019**, *42* (3), 650–661.
- (36) Zhou, X.; Liang, G. Y.; Wang, D. P.; et al. [Study on the chemical constituents of the volatile oil from *Lysimachia paridiformis* var. *stenophylla* Franch.]. *Se Pu* **2002**, *20* (3), 286–288.
- (37) Chen, L.; Li, J.; Ke, X.; et al. The therapeutic effects of *Periploca forrestii* Schltr. stem extracts on collagen-induced arthritis by inhibiting the activation of Src/NF- κ B signaling pathway in rats. *J. Ethnopharmacol.* **2017**, *202*, 12–19.
- (38) Chen, L.; Tang, S.; Li, X.; et al. A review on traditional usages, chemical constituents and pharmacological activities of *periploca forrestii* schltr. *J. Ethnopharmacol.* **2021**, *271*, No. 113892.
- (39) Ye, F.; Mo, X. H.; Hu, T. T. Effect of Clascoterone on proliferation, lipid synthesis, and expression of inflammatory factors in SZ95 human sebaceous gland cells. *China J. Lepr. Skin Dis.* **2022**, *38* (06), 349–354.
- (40) Marbach-Breitrick, E.; Rohwer, N.; Infante-Duarte, C.; et al. Knock-In Mice Expressing a 15-Lipoxygenating Alox5 Mutant Respond Differently to Experimental Inflammation Than Reported Alox5(–/–) Mice. *Metabolites* **2021**, *11* (10), No. 698, DOI: 10.3390/metabo11100698.
- (41) Zimmermann, S.; Peters, S. Going beyond EGFR. *Ann. Oncol.* **2012**, *23* (10), 197–203.
- (42) Baker, J.; Falconer, A. M. D.; Wilkinson, D. J.; et al. Protein kinase D3 modulates MMP1 and MMP13 expression in human chondrocytes. *PLoS One* **2018**, *13* (4), No. e0195864.
- (43) Mu, X.; Bellayr, I.; Pan, H.; et al. Regeneration of soft tissues is promoted by MMP1 treatment after digit amputation in mice. *PLoS One* **2013**, *8* (3), No. e59105.
- (44) Liu, G. M. *Studies on Anti-Inflammatory and Metabolic Mechanism of Hypermaloside In Vitro*; Changchun Normal University, 2022.
- (45) Sophocleous, A.; Marino, S.; Kabir, D.; et al. Combined deficiency of the Cnr1 and Cnr2 receptors protects against age-related bone loss by osteoclast inhibition. *Aging Cell* **2017**, *16* (5), 1051–1061.
- (46) Brunello, L. AR in immunotherapy. *Nat. Rev. Cancer* **2022**, *22* (6), No. 319.
- (47) Bendre, M.; Comasco, E.; Nylander, I.; Nilsson, K. W. Effect of voluntary alcohol consumption on Maa expression in the mesocorticolimbic brain of adult male rats previously exposed to prolonged maternal separation. *Transl. Psychiatry* **2015**, *5* (12), No. e690.
- (48) Zhang, Z. Z. *Identification of Differentially Expressed Mirnas and Functional Study of gga-miR-15a in Broaching Chicken with Limb Varus and Valgus Deformity Leg Sisease*; Henan Agricultural University, 2022.
- (49) Che, C.; Liu, J.; Ma, L.; et al. LOX-1 is involved in IL-1 β production and extracellular matrix breakdown in dental peri-implantitis. *Int. Immunopharmacol.* **2017**, *52*, 127–135.
- (50) Daneault, A.; Prawitt, J.; Soulé, V. F.; et al. Biological effect of hydrolyzed collagen on bone metabolism. *Crit. Rev. Food Sci. Nutr.* **2017**, *57* (9), 1922–1937.
- (51) Minton, K. Extracellular matrix: Preconditioning the ECM for fibrosis. *Nature reviews. Mol. Cell Biol.* **2014**, *15* (12), 766–767.
- (52) Schadow, S.; Siebert, H. C.; Lochnit, G.; et al. Collagen metabolism of human osteoarthritic articular cartilage as modulated by bovine collagen hydrolysates. *PLoS One* **2013**, *8* (1), No. e53955.
- (53) Champiat, S.; Dercle, L.; Ammari, S.; et al. Hyperprogressive Disease Is a New Pattern of Progression in Cancer Patients Treated by Anti-PD-1/PD-L1. *Clin. Cancer Res.* **2017**, *23* (8), 1920–1928.
- (54) Malemud, C. J. Intracellular Signaling Pathways in Rheumatoid Arthritis. *J. Clin. Cell. Immunol.* **2013**, *04*, No. 160.
- (55) Hou, Q.; He, W. J.; Wu, Y. S.; et al. Berberine: A Traditional Natural Product With Novel Biological Activities. *Altern. Ther. Health Med.* **2020**, *26* (S2), 20–27.
- (56) Wang, Y.; Zhou, X.; Zhao, D.; et al. Berberine inhibits free fatty acid and LPS-induced inflammation via modulating ER stress response in macrophages and hepatocytes. *PLoS One* **2020**, *15* (5), No. e0232630.
- (57) Zhu, C.; Li, K.; Peng, X. X.; et al. Berberine a traditional Chinese drug repurposing: Its actions in inflammation-associated ulcerative colitis and cancer therapy. *Front. Immunol.* **2022**, *13*, No. 1083788.
- (58) He, S. M.; Song, W. L.; Cong, K.; et al. Identification of candidate genes involved in isoquinoline alkaloids biosynthesis in *Dactylicapnos scandens* by transcriptome analysis. *Sci. Rep.* **2017**, *7* (1), No. 9119.
- (59) Zhao, Z.; Xiao, J.; Wang, J.; et al. Anti-inflammatory effects of novel *sinomenine* derivatives. *Int. Immunopharmacol.* **2015**, *29* (2), 354–360.